

PHYSICAL INSIGHTS ON SPT THRUSTERS THROUGH ULTRA-FAST , EXTERNALLY DRIVEN CURRENT INTERRUPTIONS

Vanessa Vial*, Alexey Lazurenko*, André Bouchoule* , Mathieu Prioul**

*: GREMI Laboratory, Orléans university, 45067 Orléans Cedex 2

** present adress : SNECMA , Direction Propulsion et Equipements Satellites, 77 550,Moissy Cramayel
e-mail : andre.bouchoule@univ-orleans.fr

Paper ref 0220 - 02IEPC 2003 - Toulouse, France

Abstract:

Ultrafast current interruptions of the current of a Hall thruster, with ON-OFF transit time much shorter than the characteristic time scale of its spontaneous current fluctuations, was evidenced in a previous paper as a powerful tool for physical characterizations. This paper presents results obtained on two thrusters of different design SPT 100 ML and A53 thrusters operated at similar mass flow and voltage ranges. These data have been obtained by using time resolved electrical and optical diagnostics fast enough to record transient phenomena induced by this externally induced perturbation. Insights on thruster plume, Hall electron current, electron current at thruster channel input are shown as throughputs of this approach, allowing some comparisons between these two thrusters.

Introduction

In the previous years the development of time resolved diagnostics induced significant insights on dynamic phenomena involved in spontaneous fluctuations-oscillations of Hall thrusters (ref : 1,2). Among the new results derived from such studies was the evidence of transient angular and energy distributions in the plume of an SPT 100 ML thruster directly related to thruster current fluctuations . It was evidenced that the time averaged data on ion energy distribution in the thruster plume was not really significant in terms of thruster physics. The observed broadening is in fact mostly due to a time varying energy spectrum which is at each time a rather narrow one with FWHM value lower than 30 eV. So, the significant output of such data is that the ionization occur in a rather well defined plasma layer where the potential drop remains in this range of 30 eV while the mean value of this potential is a time varying one.

It is well known that a fruitful approach for studying any physical system is to use impulse perturbations, at time scales much shorter than the characteristic time scale of the system itself. For linear systems this approach is equivalent to a frequency analysis through Fourier transform. Such ultrafast externally driven perturbation has been developed by GREMI laboratory in order to acquire new experimental insights in Hall thruster physics. It was shown previously that Hall thruster discharge behaves as an almost pure current noise source for fluctuating or oscillating regimes (ref 3). It means that only a current perturbation can be relevant. The easiest way was to impose ultrafast current interruptions by using an optically driven fast MOSFET installed on the anode wire between the DC supply and the thruster. Technical details are given in part I and the meanings of the label « ultrafast » for this externally driven perturbation is evidenced in terms of physical data recorded at the ON-OFF anode current fall.

Several results on physics of the SPT 100ML thruster, derived from various time resolved diagnostics, have been already presented (4,5,6). For example , time and space resolved spectroscopic data recorded for the channel plasma lead to new insights on atomic physics, where the impact of metastable states and two step processes for X_e and X_e^+ excited states population was evidenced. Moreover it was shown that such technique is a powerful one for plume analysis, leading to angular and energy resolved data on X_e^+ , X_e^{++} , X_e^{+++} ions (6,7)

In the part II of this paper new data derived from ultrafast perturbation technique will be emphasized.

- The first one concerns results obtained on the A53 thruster from SNECMA having a structure similar to the ATON thruster developed by MIREA in Moscow. A comparison with previous data obtained for SPT 100ML thruster evidences both similarities and significant differences, related to their different geometrical and magnetic design.

- The second one, derived from both optical and electrical time resolved data, concerns transient phenomena related to the electron flow emitted by the cathode and to the anode and cathode currents and voltages waveforms. It is shown that this ultrafast perturbation could give a direct access to an important physical feature which is the electron current input at the thruster channel entrance.

These data emphasize the usefulness of the ultra-fast perturbative approach for a better understanding of physical features of Hall thrusters.

PART I : technical and physical features of an externally driven ultra-fast interruption of Hall thruster current

I 1 : technical considerations

The main features of the device used for driving such current interruptions have been presented in short form previously (4). They are recalled here with some details.

Several considerations was to be taken into account when designing such device.

- the first one is a straightforward one: if a perturbation has to be considered as an ultrafast one its characteristic time should be significantly shorter than spontaneous response time in terms of system characteristics. For Hall thruster discharges it means that the ON-OFF and OFF-ON transitions should occur in a faster way than the discharge plasma relaxation. This characteristic time related to the discharge plasma is defined by the well known ionisation instabilities whose typical frequencies are in the 10-20 kHz range. It means that external perturbations should involve electrical transients with durations less than one microsecond.
- The second one, as explained above, is that only a thruster current perturbation is relevant
- The third one is related to specific considerations of the thruster currents. In the configuration used for these studies, performed in the PIVOINE facility (8), the electrical supply and the thruster electrodes are floating with respect to ground (vacuum tank). The thruster anode is at the bottom of the insulated annular channel, where a transverse magnetic field acts as an electron current barrier. The hollow cathode is external, acting as source of primary electrons entering the channel and as a source of the electrons achieving the plume neutralization.. This last contribution is the most important one : the highest is its percentage, the lowest is the thruster current and the highest its efficiency. A current interruption of the anode current is a well defined phenomenon, with a cancellation of the current everywhere in the channel at the ON-OFF externally driven rate. Inversely a current interruption of the cathode current is a complex process, this electrode connected to the vacuum tank through the plasma induced by cathode electrons and thruster plume. The first experiments evidenced clearly the strongly different transients observed when anode or cathode currents interruptions was compared. All experiments have been made by using a fast power electronics switch installed on the anode feeding wire.
- The last consideration is related to the floating peculiarity of the electrical thruster circuit. It means that an optically driven switch was required.

The overall electrical configuration design is shown figure 1.

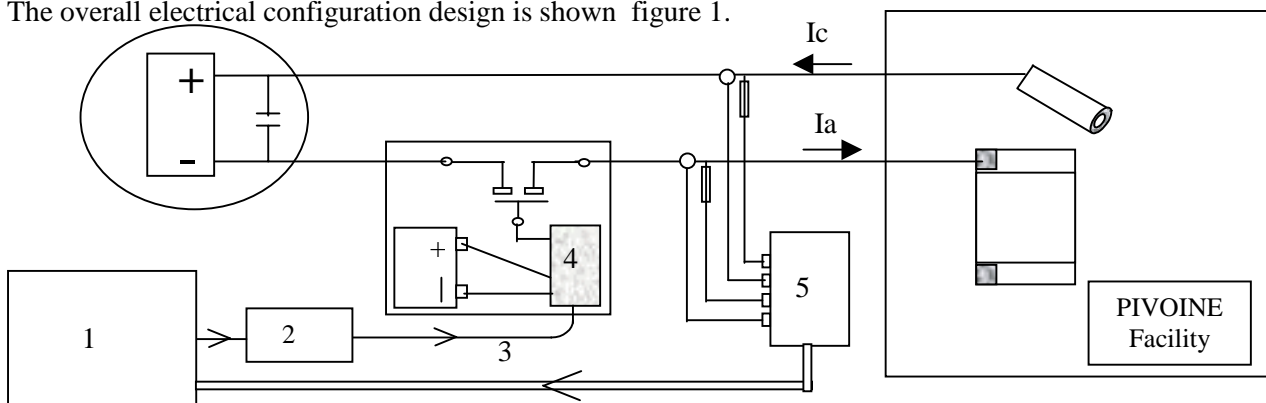
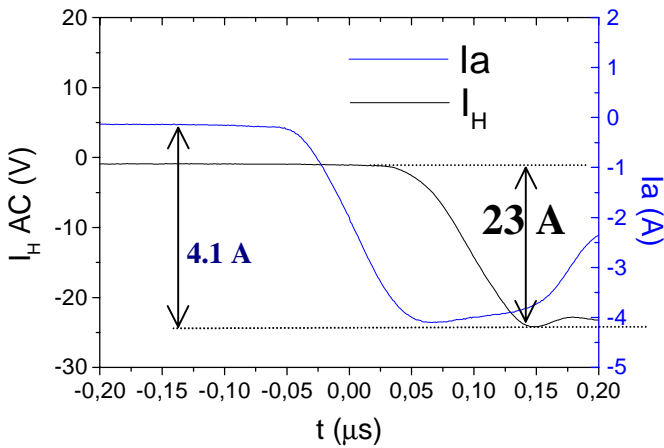


Figure 1

A computer (1) controlled programmable pulse generator (2) drives through an optical fiber (3) a galvanic isolated power MOSFET switch installed on the anode wire. The same computer is used to record time data of an oscilloscope. In the configuration shown these data are current and voltage signals given by wide-band Tektronix probes. The ON-OFF and OFF-ON transition of the switch are less than 200 ns (ref).

I 2 : physics of ON-OFF transients



The transient phenomena induced at anode current interruption have been investigated through several diagnostics (9). Results obtained by time resolved LIF and electron drift current Hall probe are discussed below.

A single turn loop is installed in a groove, managed near its exit, around the ceramic channel. The loop signal is used to measure the variations of the electron drift Hall current. This diagnostic was calibrated by using a copper wire simulating the annular electron current both in harmonic and fast transient regimes. For the SPT 100ML thruster, at nominal working point (5 mg/s, 300 V, 4.3 A, 82 mN) the measured

electron drift current was 23 A as obtained through studies of spontaneous fluctuations of discharge current. The figure 2 shows the transient signals of anode current and Hall probe. The ultrafast cancellation of the discharge current is accompanied by a simultaneous ultrafast cancellation of the electron drift current as evidenced by the drift current drop of 23 A, as derived from calibration data. Spectroscopic data show that the electron density is decreasing at the much lower rate, in few μs . It means that the electric field driving the drift current in the channel experience also an ultrafast decay at anode current interruption. As the electron contribution to the total channel current is also cancelled, it means that the ion flow leaving the channel should be stopped in an ultrafast way. Such very fast drop of the ion flow has been evidenced by using time resolved LIF on an SPT 50 thruster in cooperative experiment (N. Sadeghi LSP Grenoble, J. Bonnet, ONERA Palaiseau, M. Prioul. GREMI). Details on this experiment, involving photon counting techniques as probed previously on ion source (10), can be found in paper presented by J. Bonnet & N. Sadeghi at IEPC 2003.

The figures 3 and 4 below show the experiment design and a result obtained when the laser frequency is adjusted to probe the ion flow density at the maximum values of its velocity distribution function.

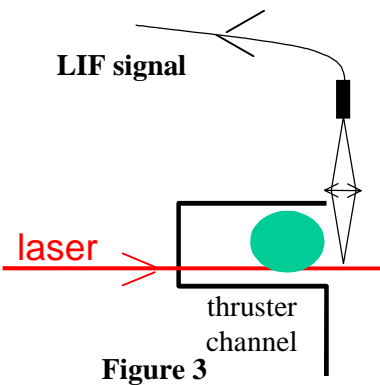


Figure 3

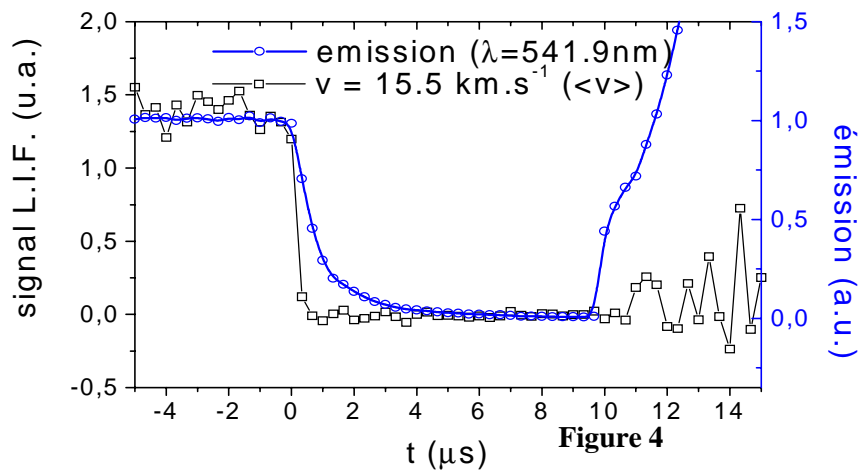


Figure 4

The result shown on figure 4 was obtained with a time resolution of the multi-channel system recording LIF photon in the photon counting mode was 300 ns. The observed drop of the energetic ions leaving the SPT thruster is achieved at the ultrafast rate, as previously expected. It means that this ultrafast cancelling of the ion beam source allows the use of time of flight techniques for studying the ion beam launched by the thruster in the plume. An RPA, at 60 cm of the channel exit records the overall drop of the ion signal and single, double or triple charge Xe ions are characterized by successive contributions of these ions in this signal drop. As energy filtering is available and as the RPA can scan various angular directions, this technique is an unique one able to give angular and energy informations on the various ions contributions in the thruster plume.

Data relevant of the use of such diagnostics for SPT 100 ML thruster was already published (9). The same technique has been applied to similar study for the A53 thruster, as shown in part II.

Finally the last remark is connected to time scale considerations. The final velocity of ions in the plume is acquired after the channel exit, at few cm (11). This velocity is close to $1.8 \cdot 10^4 \text{ ms}^{-1}$ at the nominal operating point of the SPT 100ML. The time required for the disappearance of the fast ions in the plume is of the order of $3 \mu\text{s}$ at 6 cm from the channel exit, i.e much longer than the cancellation of the electron current everywhere in the channel. It means that the part of the electron flow leaving the cathode and entering the channel should be faster cancelled or faster restored than the part involved in the neutralization of the ion plume flow. It means that a direct information could be obtained on these two contributions to the cathode current. This is an important issue for thruster performances and difficult to be derived by any other approach. This point will be discussed also in part II.

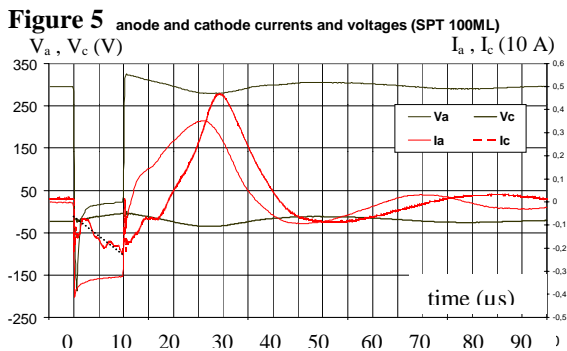
PART II : physical insights on SPT 100ML and A53 thrusters.

II 1 : Details on the electrical behavior : currents and voltages

A full set of data (anode and cathode currents and voltages) acquired on the SPT 100ML thruster operated at it's nominal working point and under the application of a $10 \mu\text{s}$ anode current interruption was acquired. The signals shown on figure 5 emphasize some characteristic features for the current and voltage waveforms. Strong differences are evidenced on anode and cathode currents and voltage transients and are discussed below.

II 1 : currents and voltages data

II 1 a : electrodes voltage signals (SPT 100 ML) - evolution in the current interruption phase

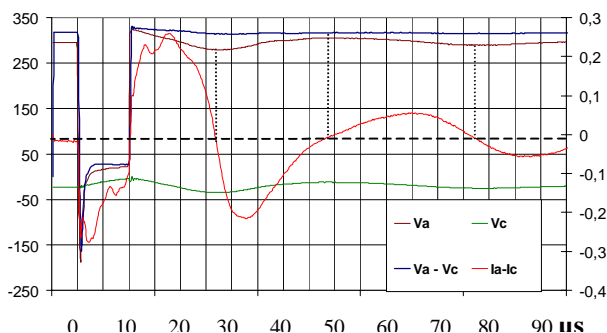


The cathode voltage is smoothly decreasing from the initial stationary value (-19V) towards near zero during the interruptions time $10 \mu\text{s}$. This behavior is expected as the thruster cathode is electrically related to the large volume plasma of the grounded PIVOINE facility. The plasma potential, defined by the electron temperature through the sheath potential drop, remains constant at first approximation and the cathode potential is related to the cathode current injected in the PIVOINE plasma., whose variations are also smooth ones.

The anode potential evidence a strong (-250 V) and very short ($<1 \mu\text{s}$) negative jump. This jump is clearly connected to the cancellation of the thruster channel current. The electron current input on to this electrode is 4 A just before opening of the switch and the anode potential jump occurs during the cancellation of this electron flow. The voltage transient is related to an equivalent capacitance of the anode line. Taking into account the above data this capacitance can be estimated to $C_{\text{aeq}} \approx 0.5 \text{ nF}$.

- evolution after OFF-ON switching

Figure 6 : anode and cathode currents and voltages (SPT 100ML)



The anode potential is restored, through a fast positive jump, at it's stationnary value, while the cathode potential is smoothly also growing to the permanent value. Later on these two potentials experience similar and small oscillations. When looking at the anode and cathode currents it is clear that these common voltage oscillations appear as induced by the overall charge flow leaving the thruster (anode + cathode current)

The figure 6 shows the evolution of this total charge flow and the common voltage oscillation. The PIVOINE plasma potential being assumed almost constant these oscillations of the floating thruster potential can also be described by defining an

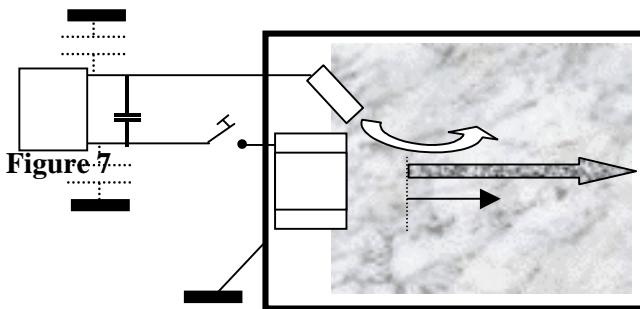
equivalent capacitance between the whole thruster structure and this plasma. Taking into account current and voltage data of figure 6 this capacitance value is $C_{Theq} \approx 1 \mu F$.

This oscillations of the thruster floating potential show that electron flow and ion flow launched in the plume have not the same instantaneous value. This feature will be discussed below.

II 1 b : electrodes current signals during current interruptions (SSPT 100ML)

The cathode current exhibit fast transients superimposed on a smooth decrease. As was shown in Part I the fast electron current interruption within the channel suggests that the electron current input from the cathode should also be cancelled in a fast way. The amplitude of this drop was tentatively deduced from the extension of the smooth evolution at the ON-OFF transition of anode current, shown by the dotted line on figure 5. The corresponding value is $\cong 20\%$ of the full initial cathode current. This determination appear to be consistent with indirect estimations. Further investigations remain required in order to confirm the validity and precision of such a direct measurement of the electron current at the channel input. It's great interest would be evident both in terms of thruster quality and for comparison with simulations.

After the fast initial transient a smooth relaxation of both cathode current and voltage is observed, at zero anode current and negligible potential difference between anode and cathode. It means that a capacitive-like current path between cathode and ground is involved, as shown on figure 7. The equivalent capacitance C_{ceqq} is derived from current/voltage data in this period. The cathode voltage drop is 18 Volts and the average



remaining a negative one (-20 \rightarrow -2 V) it is clear that cathode emit electrons in the facility plasma. If these electrons was stored (during this 10 μs step) the average density increase in the facility would be of the order of 10^7 cm^{-3} . Even if this value is small enough, such an accumulation of electrons is not consistent with the decrease of the total number of plume ion in the facility plasma.

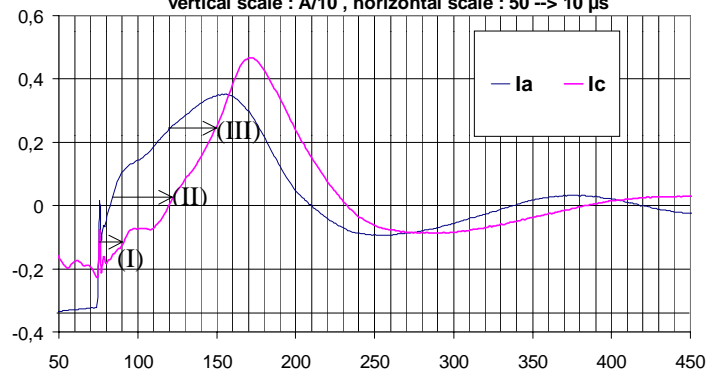
II 1 b : currents after discharge OFF-ON transition (SPT 100 ML)

Figure 8 shows anode and cathode signals.

The initial transient peak was shown to be connected to the low density plasma left in the thruster channel (ref). This density is low after 10 μs current interruption. The excess of neutrals injected trough the anode during current interruption leads to an ionization burst starting from external electrons. Details on the dynamics of this ionization was obtained by using an array of optical fibers viewing the channel length. The result is that this "ionization wave" moves at a typical velocity of the order of 10^3 ms^{-1} towards the anode. As the main part of cathode current is used for plume neutralization and as there is a variable delay between ionization and presence of accelerated ions in the plume, a detailed explanation of the current signals is not trivial. Besides the very short initial peak the growth of the recorded currents appear in three steps which appear to be connected with different delays and different amplitudes. One of the most interesting features in this representation is the evidence of a characteristic delay of 1.5 – 2 μs between anode and cathode maximum.. Taking into account that ions are accelerated at 16-18 km s^{-1} it means that the ion flow current is at neutralized by the electron flow (emitted by the cathode) at a distance of the order of 8-10 cm of the channel exit.

cathode current is 2.5 A in this 10 μs interval. The corresponding value of C_{ceqq} is 1.4 μF , of the same order as the capacitance derived above for describing the evolution of the floating potential of the thruster after the OFF-ON transition of the switch. current It's value is of the order of 3 μF . Finally it should be mentionned that the plasma potential is defined by the electron temperature and cannot be modified significantly in this period. The cathode potential

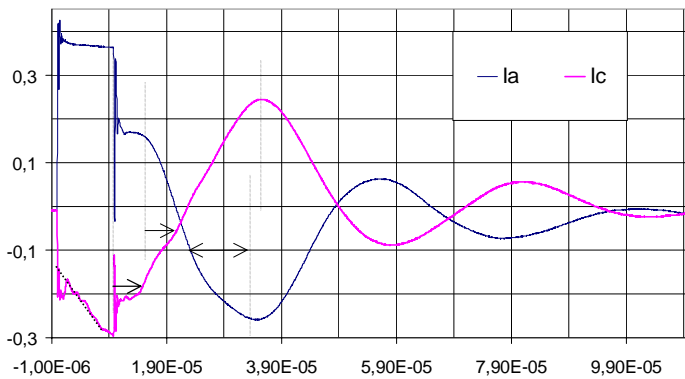
Figure 8 anode and cathode currents after OFF-ON switch transition
vertical scale : A/10 , horizontal scale : 50 \rightarrow 10 μs



II 1 c : comparison between thrusters SPT 100ML and A53

Anode and current signals recorded for an A53 thruster are shown Figure 9. For this thruster only current signals was available. The operating parameters was $4.6 \text{ mgs}^{-1} \text{Xe}$, 348 V, 3.96 A. As for SPT 100ML thruster the anode line switch was open for $10 \mu\text{s}$.

Figure 9 anode and cathode currents (A53)



A rather similar behavior is observed but some differences with SPT 100 MI behavior are evidenced :

- the maximum amplitude of the anode current burst is 6.3 A while it was 9 A for SPT 100ML.

- When using the same method for an estimation of the electron current at the channel entrance a higher contribution is

obtained : up to 30% of the total cathode current !

- Finally the burst of anode current appear with a longer delay after OFF-ON switching : $26 \mu\text{s}$ in place of $16 \mu\text{s}$ for SPT 100ML.

The difference on amplitude of current bursts is clearly related to the difference of the shapes of these two thrusters. The gas flow is confined in the channel it-self in the SPT structure while a comparatively large volume is managed downwards the annular anode in A53 structure. It means that the same amount of neutral gas injected in the A53 leads to a less significant increase of the neutral density in the thruster channel. The switch effect appear as a relatively low perturbation in this situation.

The second result is surprising: such a high value of the electron current contribution is not expected. As discussed previously this diagnostic needs more specific studies to be an unambiguous one.

The last result is consistent with the dynamics of the ionization burst progressing towards anode in both configurations: a reduced speed value, by a factor 0.62, was estimated from time resolved optical measurements in the situation of A53 thruster (7) . This point is significant in terms of thruster stability against ionization fluctuations : the neutral velocity is close to the ionization wave velocity for A53 thruster and significantly lower for SPT 100 ML thruster. It means that neutral depletion-refilling phenomena can be developed more easily in SPT than in A53 thruster, as it is observed.

II 1 d : Impact of interruption duration on thruster behavior

The figure 10 presents two set of recordings of the anode current in SPT and A53 thruster for various switch interruptions durations.

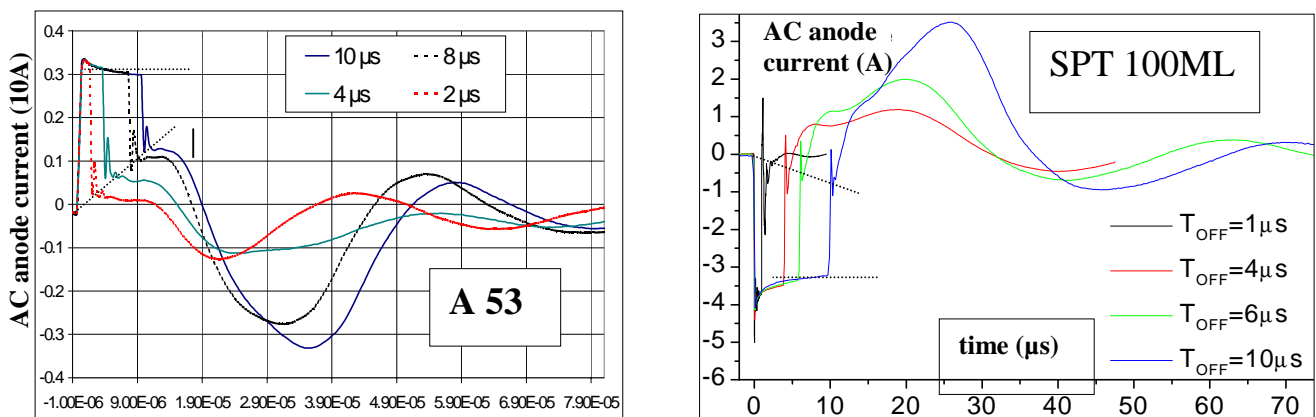


Figure 10

A roughly similar evolution is observed for these two thrusters, with a three step evolution after OFF-ON switching. But significant differences can be underlined :

- the amplitude of the instantaneous transient peaks of current decreases in a faster way for the A53 thruster.
- For all OFF durations the stepwise evolution is much more clearly evidenced than for SPT thruster and the relevant anode current (DC) has lower values for A53 than for SPT thruster.

- On A53 data it is clear that the initial plateau has a longer duration for shorter OFF periods. The first one suggests that the internal plasma relaxation (recombination on walls) is faster for A53 thruster. The second and third ones are consistent with previous remarks : faster decrease of plasma density in the OFF period and slower velocity of ionization propagation towards anode for the A53 thruster.

I 2 : Data derived from time resolved fast camera picture

I 2 a. Diagnostics details

Short exposure ($0.1\mu\text{s}$) images for outer channel plasma have been obtained by using an ICCD camera controlled by a pulse generator (a pulser). The camera was installed perpendicular to the thruster axis at the distance of $\sim 2\text{m}$. The pulser was synchronized with the above described interrupter. By the use of optical filters images corresponding to ion or neutral spectral emission can be obtained. Evolution in time of this emission was tracked by taking the images with $1\mu\text{s}$ time step.

I 2 b. Studying of the extinction of the discharge

Evolution of the outer plasma luminescence during the phase of the discharge extinction was tracked by the collecting the light without filter and with the filters 450nm (ion metastables), 525nm (ion metastables) and 825nm (neutral metastables). It was observed that characteristic time of ion luminescence decrease is shorter than that of neutrals (Fig. 11). Over the interval of $3\mu\text{s}$ ion luminescence intensity drops at one order of magnitude till the value only 3 times greater than the background luminescence. At the same time intensity of neutral luminescence remains on the considerable level of more than one order of magnitude greater than the background luminescence. These values correspond very well to the characteristic times of the relaxation of the corresponding spectral lines [7]. During the first $2\mu\text{s}$ after current interruption, when there is enough ion luminescence, there was not observed any displacement of the region with maximal luminescence.

I 2 c. Studying of the ignition of the discharge

During the discharge ignition we observed a propagating from the thruster front of the luminescence (Fig.12) with a velocity $\sim 13\text{ km/s}$. Assuming that this is a front of accelerated ions and comparing its velocity to the nominal ion exhaust velocity $\sim 18\text{ km/s}$ [11] one can draw a conclusion that ionization begins closer to the exit of the thruster (comparatively to the position of the ionization zone during stationary operation as was already shown by using time-resolved RPA diagnostics [1]). That is why ions at the ignition do not undergo the total potential difference. Further investigation of the intensity profiles reveals the fact that maximum of the luminescence at the exit of the thruster is reached $\sim 7\mu\text{s}$ earlier than maximum of the discharge current. If we assume that luminescence intensity at each space point is proportional to the product of electron and metastable ion number densities then the maximum of luminescence corresponds to the maximum of these values. Then this time interval can give an estimation of characteristic time of electron propagation towards the anode. This conclusion is supported by the fact that there was not observed any time shift between the luminescence and discharge current maximums at the exit of the cathode. But of course this phenomenon needs further studies.

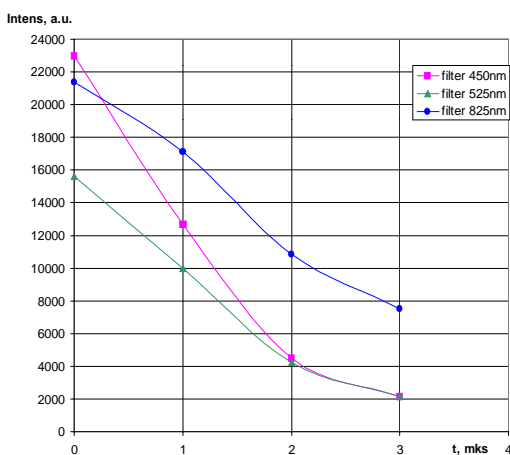


Fig. 11 Evolution of the ion and neutral luminescence during extinction of the discharge

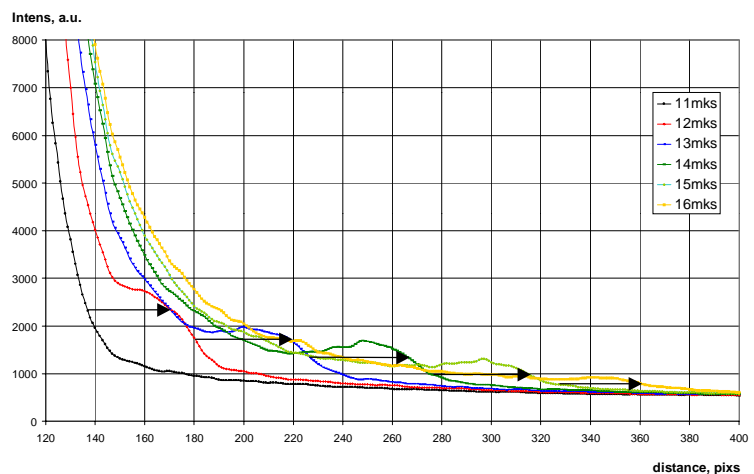


Fig. 12 Evolution of the profiles of luminescence intensity at the middle radius of the channel (out of the thruster)

I 3 : data derived from transient RPA signals

The time of flight technique has been already used for characterization of the Xe^+ , Xe^{++} contributions in the plume of the SPT 100ML (relative currents, energy and angular distributions). Significant differences have been evidenced for the A53 thruster with an RPA located at 60 cm from the thruster channel output.

The figure 13 shows RPA collector current recorded for various directions referred to the axis of the A 53 thruster. The ON-OFF switch transition is the origin of the horizontal time scale. The figure 14 is a detailed view corresponding to the thruster current extinction. The oscillations of figure 13 reflect discharge current oscillations following the discharge interruption while figure 14 gives insights on ion velocity distribution ,as seen at a constant distance supposed to be 0.6 m of thruster exit, before current interruption.

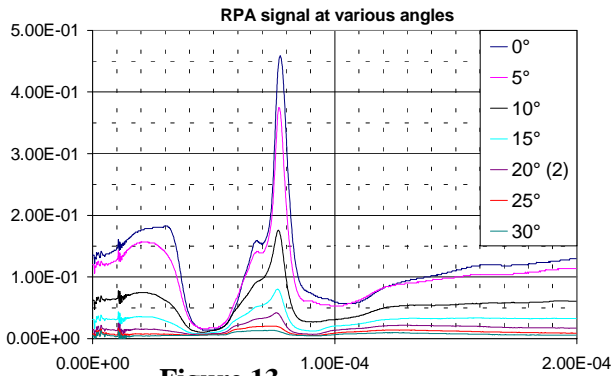


Figure 13

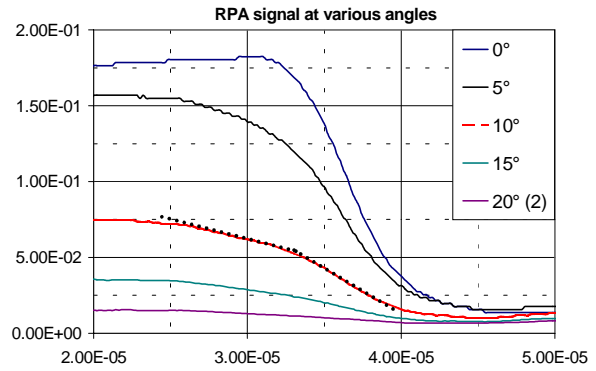


Figure 14

The RPA current fall on figure 14 has significant differences with typical signal recorded at 0° for the SPT 100 ML thruster as shown on figure 14bis [9].

The main difference is a much less clear evidence of single and multiple charge ions in the signal drop.

Nevertheless a rough decomposition of the A53 signal drop in two components is possible, as shown on the signal recorded at an angle of 10° .

From the corresponding velocity range and current contributions the kinetic energy and relative current contribution of these two components was obtained and are reported on the table below.

The assignment of these two components to single and double charge Xe ions leads, at first, to surprising data in terms of energy

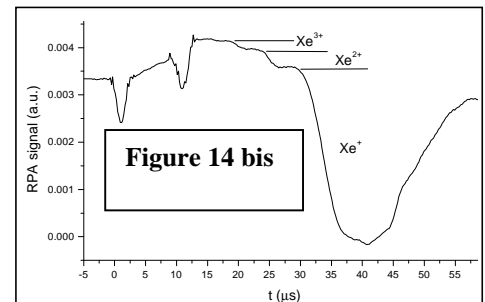


Figure 14 bis

Angle (°)	Ion ??	Em	E-	E+	I ⁺	I ⁺⁺	η_I	η_F
0	Xe^+	185	215	165	0.165			
5	Xe^+	190	215	170	0.0974		31	18
5	Xe^{++}	290	335	240		0.044		
10	Xe^+	190	215	165	0.0358		36	22
10	Xe^{++}	290	350	240		0.0204		
15	Xe^+	185	220	165	0.027		34	20
15	Xe^{++}	290	340	250		0.014		
20	Xe^+	185	220	165	0.0046		50	33
20	Xe^{++}	290	340	250		0.0046		

ranges (cf ref 12 , 13). For the discharge voltage of 300 volts, Xe^+ energy is expected to be near 250 Volts. In fact these data, derived from time of flight delays, would be close to expected values if the time of flight path was 0.7 m in place of 0.6 m. It could be an artefact of the computer driving RPA and thruster positions.

Anyway the comparison with SPT 100ML data is consistent in terms of the contribution of double charge ions in the plume . η_I is the current contribution derived for A53 thruster and this contribution was 15% to 50% for SPT 100ML (0-25° angular range (9).

Further experiments are clearly required to be sure of the results on A53 thruster. The figure 15 shows the evolution of the RPA current as function of the RPA voltage at two times after the OFF-ON switch transition.. They confirm also that the RPA signal in this period is a complex one, involving more complex energy distributions.

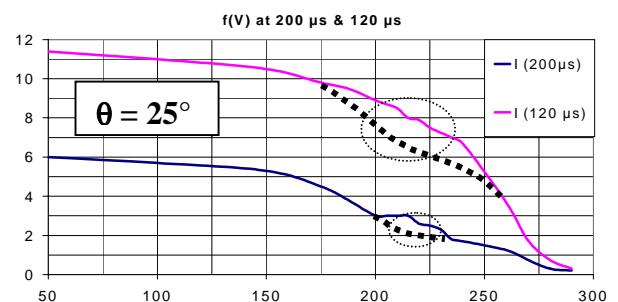
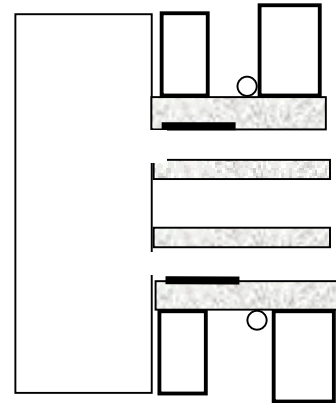


Figure 15

I 4 : Electron Hall current measurements.

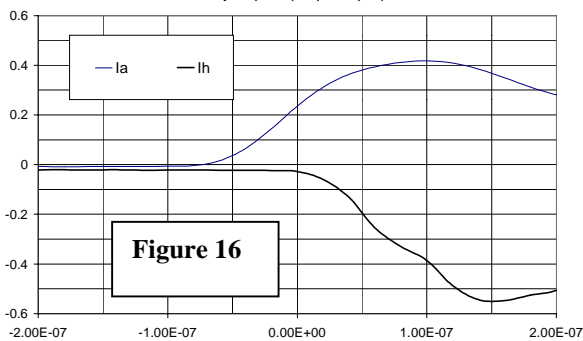
The determination of the azimuthal electron drift current has been achieved as explained in part I. This measurement imply first a calibration by using a copper loop for simulation of the Hall current, with a ON-OFF current drop driven by the same switch. The diagnostic antenna was wounded around the ceramic channel of the A53 , but, due to its configuration the only available position was as schematically shown in the drawing. Both anode and magnetic external coils represent electromagnetic shields . This peculiarity leads to a high sensitivity of the calibration as function of the copper loop position along the channel. Such shielding did not exist for the SPT 100ML and it was found that the antenna signal was not sensitive to the excitation loop position.



The copper loop was displaced between channel exit (0) and anode border (20). The antenna signal is the amplitude of the fast signal jump when the current excitation current fall down from 23.5 A.

The measured antenna signal was recorded for the standard operating point of A53 (current of 4.2 A) and is shown on figure 16.

Position (mm)	0	5	10	15	20
Loop signal (V)	0.54	0.84	1.55	2.43	3.95



As for the measurements on the SPT 100ML, an ultrafast drop is observed for the antenna signal and the discharge current. The amplitude of the Hall current itself cannot be deduced, as the calibration shows that the antenna signal is strongly dependent on the electron drift current position. As shown in part I , the Hall current of SPT 100MI was measured without such a problem and was of 23 A for a discharge current close to the A53 discharge current. As the antenna signal vary I a rather fast way as function of the azimuthal current position, and assuming that the electron drift current remains close to the SPT

100 value we can infer that the main electron the drift current density of the A53 thruster is installed near the channel exit.

CONCLUSION :

The approach of ultrafast interruptions of anode current was developed at GREMI laboratory in order to derive new insights on physical characteristics of closed electron drift thrusters. It opened the way to several new diagnostics whose results on SPT thrusters have been already been published

- determination of the electron drift current
- detailed analysis of the contribution of single and multiple charge ions in the plume : relative contribution , variation with angular direction, energy distribution
- dynamics of ionization phenomena and insights on atomic physics in the channel and plume

In the present paper this approach was extended to another thruster and reveals both similarities and significant differences in terms of dynamics of switch induced phenomena. Several features seems to differ also in terms of electron input in the thruster channel, kinetic energies and percentage of double charge electrons. Finally, fast camera images are shown to be a powerful tool to look at transients of the external plasma for ON-OFF and OFF-ON transitions.

Besides it's unique possibility in obtaining detailed data on the Xe^+ , Xe^{++} , Xe^{+++} ions in thruster plume one of the specific interest of this method could be to give a direct determination of the electron current at the channel input of closed electron drift thrusters. Such determination has been made up to now through indirect determinations and with a relatively poor reliability. A better determination of the electron current at the channel input would be of course welcome as an useful input for modeling and simulation studies [14].

Acknowledgements :

This work was achieved and supported by the French research organization GDR N° 2232 (CNES/CNRS/SNECMA/ONERA) and Orléans University. Mrs V. Vial and Dr A. Lazurenko are supported by grants from CNES. Experiments have been made by using the national research facility PIVOINE operated by Dr Lasgorceix, at Aérothermique laboratory Orléans.

References :

- [1] Philippe-Kadlec C., Laure C., Bouchoule A., 33th AIAA/ASME/SAE/ASEE Joint Propulsion Conference and Exhibit, Seattle (1997)
- [2] Darnon F., Philippe-Kadlec C., Bouchoule A., Lyszyk M., “Dynamic Plasma and Plume Behavior of SPT Thrusters”, AIAA 98-3644, 34th AIAA/ASME/SAE/ASEE Joint Propulsion Conference and Exhibit, Cleveland (1998).
- [3] Darnon F., Phd Thesis, Orléans University (1999).
- [4] Prioul M. , Roche S. , Pagnon D., Magne L., Touzeau M., Bouchoule A., Lasgorceix P., “Insight on Closed Electron Drift Thrusters obtained with a Discharge Shutter as Diagnostic Tool”, AIAA-2001-3358, 37th AIAA/ASME/SAE/ASEE Joint Propulsion Conference and Exhibit, Salt Lake City (200).
- [5] Bouchoule A.; Philippe-Kadlec C.; Prioul M.; Darnon F.; Lyszyk M.; Magne L.; Pagnon D.; Roche S.; Touzeau M.; Bechu S.; Lasgorceix P.; Sadeghi N.; Dorval N.; Marque J.P.; Bonnet J., “Transient phenomena in closed electron drift plasma thrusters: insights obtained in a French cooperative program”, Plasma Sources Science and Technology, may 2001; 10 (2) : 364-377.
- [6] Touzeau M.; Prioul M.; Roche S.; Gascon N.; Perot C.; Darnon F.; Bechu S.; Philippe-Kadlec C.; Magne L.; Lasgorceix P.; Pagnon D.; Bouchoule A.; Dudeck M., ”Plasma diagnostic systems for Hall-effect plasma thrusters”, Plasma Physics and Controlled Fusion, Dec. 2000; 42 Suppl. 12B : B323-B339.
- [7] Prioul M. , Thesis, Orléans University, 2002
- [8] Lasgorceix P., Pérot C., Dudeck M., Beltan T., Cadiou A. “PIVOINE ground test facility for thrusters studies”, 2nd ESPC, SP-398, p687-691, Noordwijck , 1997
- [8] Béchu S., Gascon N., Roche S., Prioul M., Albarede L., Lasgorceix P., Dudeck M., “Comparison between two kinds of Hall Thrusters: SPT100 AND ATON”, AIAA 00-3524, 36th AIAA/ASME/SAE/ASEE Joint Propulsion Conference and Exhibit, Huntsville (2000).
- [9] Prioul M., Bouchoule A., Roche S., Magne L., Pagnon D., Touzeau M., Lasgorceix P. « Insights on Physics of Hall thrusters through fast current interruptions and discharge transients » paper 01-059, IEPC 2001, Pasadena, USA
- [10] Philippe Kadlec C. , PhD thesis , orléans University, 1998
- [11] Dorval N., Bonnet J., Marque J-P., Chable S., Rogier F., Lasgorceix P., Rosencher E., ; « determination of the ionization and acceleration zones in a Stationary Plasma Thruster by optical spectroscopy study : experiment and model” J. Appl. Phys. Vol 91, N°8, 2002
- [12] Morozov A.I. and Savelyev V.V. "Fundamentals of Stationary Plasma Thruster Theory", Reviews of Plasma Physics n° 21 edited by Kadomtsev B.B. and Shafranov V.D., ISBN 0-306-11064-4, Plenum Publisher, New York, (2000).
- [13] Morozov A.I., Bugrova A.I., Desyatshov A.V., Ermakov Yu. A., Kozintseva M.V., Lipatov A.S., Pushkin A.A., Khartchevnikov V.K., and Churbanov D.V., “ATON-Thruster Plasma Accelerator”, Plasma Physics Reports, vol. 23, no. 7, 1997.
- [14] Garrigues L.; Heron A.; Adam J.C.; Bœuf J.P.,”Hybrid and particle-in-cell models of a stationary plasma thruster”, : Plasma Sources Science and Technology, 9 (2) : 219-226 (2000).